

Marco Neri · Valerio Acocella · Boris Behncke

The role of the Pernicana Fault System in the spreading of Mt. Etna (Italy) during the 2002–2003 eruption

Received: 7 February 2003 / Accepted: 13 September 2003 / Published online: 5 November 2003
© Springer-Verlag 2003

Abstract Flank instability and collapse are observed at many volcanoes. Among these, Mt. Etna is characterized by the spreading of its eastern and southern flanks. The eastern spreading area is bordered to the north by the E–W-trending Pernicana Fault System (PFS). During the 2002–2003 Etna eruption, ground fracturing along the PFS migrated eastward from the NE Rift, to as far as the 18 km distant coastline. The deformation consisted of dextral en-echelon segments, with sinistral and normal kinematics. Both of these components of displacement were one order of magnitude larger (~1 m) in the western, previously known, portion of the PFS with respect to the newly surveyed (~9 km long) eastern section (~0.1 m). This eastern section is located along a pre-existing, but previously unknown, fault, where displaced man-made structures give overall slip rates (1–1.9 cm/year), only slightly lower than those calculated for the western portion (1.4–2.3 cm/year). After an initial rapid motion during the first days of the 2002–2003 eruption, movement of the western portion of the PFS decreased dramatically, while parts of the eastern portion continued to move. These data suggest a model of spreading of the eastern flank of Etna along the PFS, characterized by eruptions along the NE Rift, instantaneous, short-lived, meter-scale displacements along the western PFS and more long-lived centimeter-scale displacements along the eastern PFS. The surface deformation then migrated

southwards, reactivating, one after the other, the NNW–SSE-trending Timpe and Trecastagni faults, with displacements of ~0.1 and ~0.04 m, respectively. These structures, along with the PFS, mark the boundaries of two adjacent blocks, moving at different times and rates. The new extent of the PFS and previous activity over its full length indicate that the sliding eastern flank extends well below the Ionian Sea. The clustering of seismic activity above 4 km b.s.l. during the eruption suggests a deep décollement for the moving mass. The collected data thus suggests a significant movement (volume >1,100 km³) of the eastern flank of Etna, both on-shore and off-shore.

Keywords Volcano spreading · Fracturing · Mt. Etna · Pernicana Fault System · NE Rift

Introduction

Flank instability is common during the lifetime of many volcanoes and can either lead to instantaneous catastrophic failure and debris avalanches or result in gravitational spreading and the episodic to continuous slippage of the unstable flank sectors (Voight et al. 1981; van Wyk de Vries and Francis 1997; van Wyk de Vries et al. 2001). Non-catastrophic volcano spreading and flank slippage has been particularly well studied at Kīlauea volcano (Hawaii) (Delaney et al. 1998, and references therein) and Mount Etna (Italy) (Borgia et al. 1992; Rust and Neri 1996; Borgia et al. 2000a, 2000b).

It is assumed that there is sometimes a very close relationship of major displacements at the unstable volcano flanks with eruptive activity. In the Kīlauea case, Ando (1979), Swanson et al. (1976) and Dvorak et al. (1986) invoke the forceful intrusion of magma into the rift zones of the volcano as the prime trigger of displacement. On the contrary, Delaney and Denlinger (1999) believe dike intrusion to be rather a surficial response to deeper-seated structural adjustments (see Parfitt and Peacock 2001 for further discussion).

Editorial responsibility: R. Cioni

M. Neri (✉)

Istituto Nazionale di Geofisica e Vulcanologia,
Piazza Roma 2, 95123 Catania, Italy
e-mail: neri@ct.ingv.it
Tel.: +39-095-7165861
Fax: +39-095-435801

V. Acocella

Dipartimento Scienze Geologiche Roma TRE,
Largo S.L. Murialdo 1, 00146 Rome, Italy

B. Behncke

Dipartimento Scienze Geologiche Università Catania,
Corso Italia 55, Catania, Italy

Since the early 1990s, research at Mt. Etna has revealed that gravitational spreading affects a large sector spanning the eastern to southern flanks of the volcano (Rust and Neri 1996, and references therein; Froger et al. 2001). Until recently, many of the processes related to the spreading, its rates, extent and causes, and its interrelationship with magmatism were poorly constrained and subject to debate (e.g. Bousquet and Lanzafame 2001).

The 2002–2003 eruption of Mt. Etna and related displacement of a large portion of its eastern to southeastern flank have provided an exceptional opportunity to constrain the unstable area and document its behavior with high precision, and to propose rough volume evaluations for the spreading portion of the volcano. We have furthermore been able to define for the first time the full length of the northern boundary of the sliding sector, known as Pernicana Fault System (PFS), and its kinematic feedback relationship with eruptive activity. Here we discuss the events pertinent to the eruption and the successive stages of displacement that yield significant insights on the dynamics of, and relationships between, flank slip, seismicity, and magma transport and eruption.

Etna volcano and the extent of spreading

Mt. Etna is the site of frequent eruptive activity, which is either focused at its four summit craters, or occurs from radial fissures that are mainly concentrated in three so-called rift zones (Garduño et al. 1997 and references therein): the NE Rift, the S Rift and the W Rift (Fig. 1). The classical model of eruptions at these rift zones envisages lateral magma drainage from the central conduit system rather than vertical magma ascent into the rift zones from depth (Kieffer 1985; McGuire and Pullen 1989; Ferrari et al. 1991; Tanguy and Kieffer 1993; Garduño et al. 1997; Bousquet and Lanzafame 2001).

Gravitational instability at Etna has been described at various scales. Small mass flows and rock falls have been reported during the 1999 summit eruption (Calvari and Pinkerton 2002). On a larger scale, the Valle del Bove depression has been interpreted to be the result of shallow-seated collapse related to the emplacement of dikes of lateral eruptions on the upper flanks (Bousquet and Lanzafame 2001 and references therein). Still on a larger scale, several studies present evidence for wholesale sliding of the eastern and southern sectors of the volcano towards E and S, respectively (Neri et al. 1991; Borgia et al. 1992; Lo Giudice and Rasà 1992; Rust and Neri 1996; Garduño et al. 1997; Borgia et al. 2000b; Froger et al. 2001). The mobile eastern portion is bordered, to the north, by the E–W-trending transtensive PFS, with a left lateral-normal motion (Fig. 1; Neri et al. 1991; Garduño et al. 1997; Tibaldi and Groppelli 2002). The sliding southern sector is confined, at its western margin, by the N–S-trending Ragalna fault system, with a predominant dextral-normal motion (Fig. 1; Rust and Neri

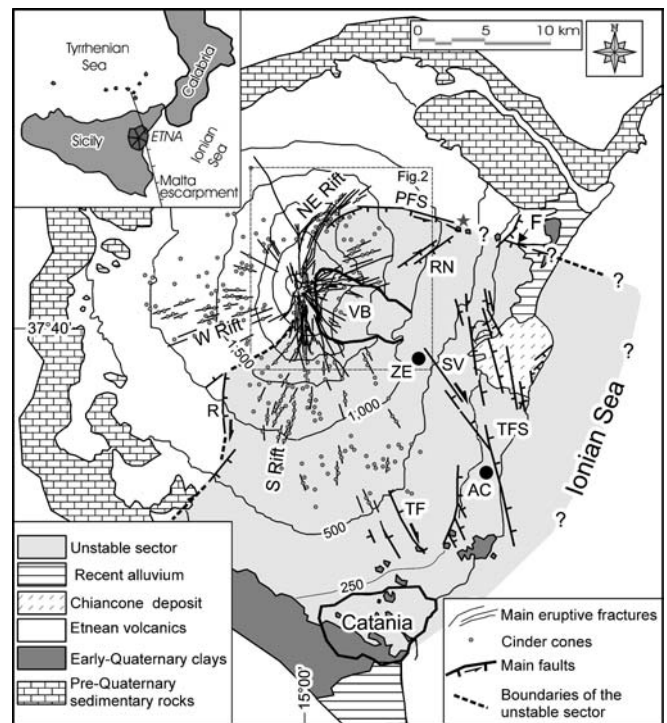
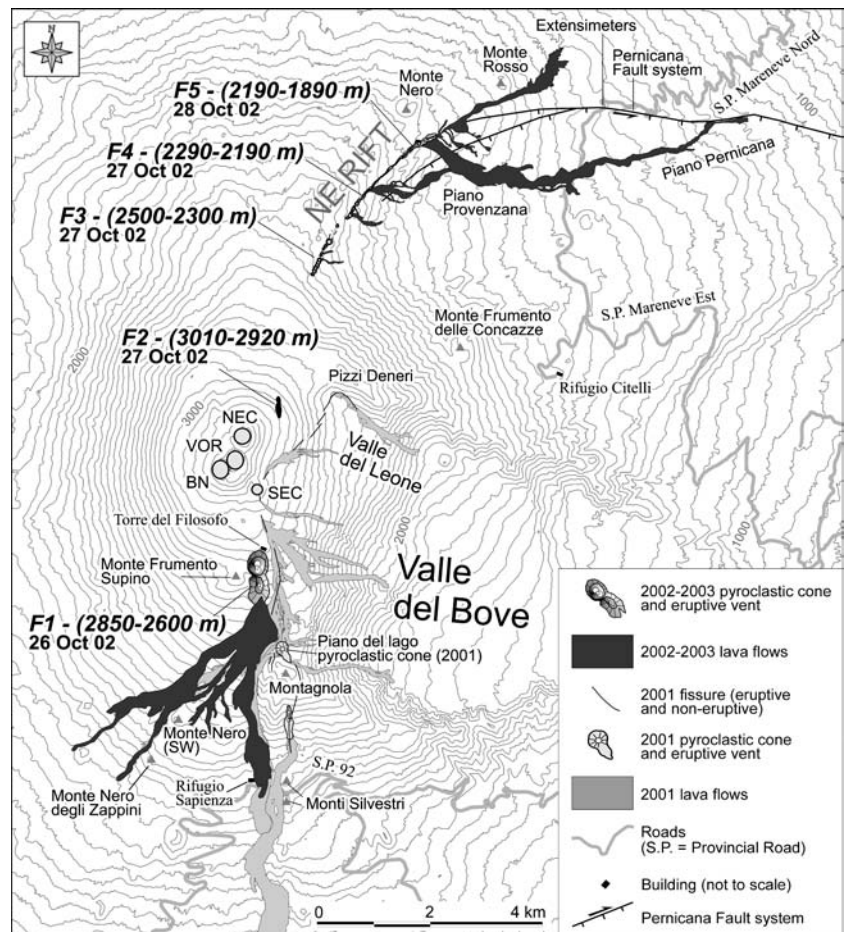


Fig. 1 Simplified geological and tectonic map of Mount Etna. The boundaries of the unstable sector of the volcano are taken from Borgia et al. (1992) and Rust and Neri (1996). The sedimentary basement is made up of units of the Apenninic-Maghrebian Chain (N and W sectors) and of early Quaternary clays (S sector). VB Valle del Bove; AC Acireale; ZE Zafferana Etnea; PFS Pernicana Fault System; F Fiumefreddo Fault; RN Ripe della Naca Faults; SV Santa Venerina fault; TFS Timpe Fault System; TF Trecastagni Fault; R Ragalna Faults. “Chiancone” deposit consisting of reworked debris avalanche deposits related to the formation of the Valle del Bove. Arrows along the faults indicate lateral component of movement. The little gray star marks the termination of PFS as known until 2002. Question marks indicate uncertainty of some boundaries of the unstable sector before 2002

1996). These two spreading areas are separated by NW–SE-trending faults, with a normal to dextral displacement, known as the Mascalucia and Trecastagni Faults (Fig. 1; Lo Giudice and Rasà 1992; Froger et al. 2001). The front of the spreading areas is probably characterized by compression leading to the formation of an anticlinal fold, which involves the sub-volcanic sediments at the southern base of the volcano and continues eastwards below the Ionian Sea (Borgia et al. 1992; 2000b).

Although there is general agreement on the surface features (identification of the structures and their kinematics) of the mobile portions at Etna, the three-dimensional extent of sliding is debated. Bousquet and Lanzafame (2001) envisage a very shallow (1–2 km a.s.l.) décollement below Etna, interpreting instability as mainly due to dike injection. A deeper décollement, between the volcanic pile and the sedimentary substratum (0–1 km a.s.l.), was proposed by Kieffer (1985) and Lo Giudice and Rasà (1992). An even deeper-seated (down to 6 km b.s.l.) décollement was assumed by Borgia et al. (1992) to be a consequence of sub-edifice magma intrusion, form-

Fig. 2 Generalized map of the 2002–2003 Etna eruption, showing the lava flows erupted from the N–S and NE-trending fissures, to the south (*F1*) and the north (*F2*, *F3*, *F4* and *F5*) of the summit craters, respectively. The westernmost portion of the PFS is shown as well



ing a plutonic complex within the sedimentary substratum. According to these models, the depth of the sliding plane is thus located somewhere between 2 km a.s.l. and 6 km b.s.l.. Recent studies suggest that both a shallow and a deep décollement can characterize, at the same time, the eastward sliding of the volcano (Tibaldi and Groppelli 2002).

The PFS is a crucial feature to characterize the style and the extent of the spreading of the eastern portion of Etna. It develops eastward from the NE Rift (from 1,850 m a.s.l.), and was known, until the 2002–2003 eruption, to extend over a length of ~9 km, partly with a prominent south-facing scarp. In its westernmost section, between 1,500 and 1,850 a.s.l., the PFS is divided into two main segments (Fig. 2), the more northerly of these starting from the Monte Nero area of the NE Rift (Garduño et al. 1997) and the more southerly from Piano Provenzana. The PFS scarp shows its maximum height of 70–80 m between 1,000 and 1,500 m a.s.l. At lower elevations (700–800 m a.s.l.), the PFS has a less defined morphological expression and is characterized by left-lateral faults with a dextral configuration. Approximately 9 km east of the NE Rift, at ~500 m a.s.l., the PFS apparently ends abruptly (marked by the grey star in Fig. 1). More than 2 km further to the east lies the ~3 km long, E–W-trending Fiumefreddo fault, which is charac-

terized by transtensive kinematics. Even though there is no evident surface connection between the PFS and the Fiumefreddo fault (Fig. 1), the latter has been commonly considered as the eastern continuation of the PFS (Lo Giudice and Rasà 1992; Azzaro et al. 1998; Tibaldi and Groppelli 2002). Shallow (<2 km) seismic activity ($2 < M < 3.5$) accompanies at times the surface deformation along the central and western portion of the PFS (Azzaro et al. 1988, 1998), while, at other times, the fault movement is characterized by aseismic creep (Obrizzo et al. 2001).

A kinematic connection of the PFS, with a feedback mechanism, to the episodic opening and eruptions of the nearby NE Rift has been proposed by various workers (Neri et al. 1991; Garduño et al. 1997; Tibaldi and Groppelli 2002; Acocella and Neri 2003). In spite of this assumed relationship, the PFS has shown continuous activity between 1947 and 2002, a period when no eruptions occurred from the NE Rift, with major surface fracturing and seismic activity in 1984–1988 (Azzaro et al. 1988).

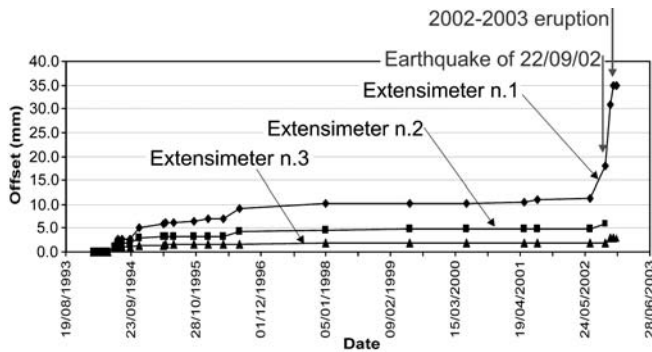


Fig. 3 Diagram showing the evolution of the deformation (since 1994) recorded by three extensimeters installed on rear side of the stone wall shown in Fig. 5 (see point 3 in Fig. 4 for location)

Structural and geological observations during the 2002–2003 eruption

Timing of events

After the July–August 2001 eruption (Accocella and Neri 2003; Behncke and Neri 2003; Billi et al. 2003; Lanzafame et al. 2003), Etna started to re-inflate in December 2001, suggesting renewed magma accumulation at 3–4 km b.s.l. (Calvari and INGV-CT scientific staff 2002). On 22 September 2002, an earthquake ($M_d=3.7$, focal depth=5 km; INGV 2002) accompanied by surface fracturing occurred along the PFS. The most evident fractures were observed at 1,450 m a.s.l., along a portion of the PFS which had been locked at least since the installation (in 1994) of extensimeters (Fig. 3; location shown in Fig. 2).

Starting at 20:25 GMT on 26 October, a seismic swarm affected the upper eastern flank of the volcano, with hypocenters between 1 and 6 km b.s.l. (Patanè 2002). During the night of 26–27 October, two fissure systems opened on the S and NE flanks of the volcano, feeding explosive activity and leading to the growth of two lava flow-fields. In particular, a 1,000-m-long N–S-trending eruptive fissure (labeled F1 in Fig. 2) opened on the upper southern flank of the volcano, at 2,850–2,600 m a.s.l. A few hours later, on the NE flank, four NE–SW-trending eruptive fissures developed from 3,010 m a.s.l. (F2 in Fig. 2), at the northern base of the NE Crater, to the lower portion of the NE Rift (F3, F4 and F5 in Fig. 2), between 2,500 and 1,890 m a.s.l. The main portion of this ~4-km-long fissure system (F3–F5 in Fig. 2) was formed by right-stepping, NE–SW-trending, en echelon segments, with moderate left-lateral shear (Table 1).

The two fissure systems showed different eruptive mechanisms and products. F1, active until 28 January 2003, produced dense, voluminous ash columns at variable rates and lava flows that extended up to 4 km S and SW (Fig. 2). After the first few days, eruptive activity focused in the upper portion of the fissure, where a cluster of pyroclastic cones grew up to 200 m high. The erupted lavas contain xenoliths of white quartzarenites

and are compositionally distinct from the products recently erupted from the central conduit system, but similar to the products of the lowermost two fissures of the 2001 eruption on the S flank (Pompilio et al. 2002). In contrast, F3–F5 on the NE Rift erupted only for 8 days and its activity was mainly characterized by effusive activity. Minor quantities of the same quartzarenite xenoliths as those within the F1 lavas were found only within a lava flow erupted on the last day of activity at F5 vent. The NE Rift lavas are compositionally similar to those erupted from the central conduit system during the past decades (Pompilio et al. 2002; Pompilio and Rutherford 2002). Behncke and Neri (2003) estimate that $\sim 30 \times 10^6$ m³ of lava and $\sim 40 \times 10^6$ m³ of tephra were erupted, of which nearly all tephra and about two-thirds of the lava came from F1 on the southern flank.

On 29 October, a seismic swarm affected the eastern flank of the volcano, damaging the village of S. Venerina (Fig. 1). The earthquakes (with $M_{max}=4.4$; 10:02 GMT) were mainly aligned along a NW–SE direction (Zafferana-Acireale trend, Fig. 1), with hypocenters located at depths of 0 to 6 km (Patanè 2002). Dextral N120°–140°-trending extensional fractures were observed in the epicentral area, with horizontal displacements exceeding 0.04 m in the town of S. Giovanni Bosco, about 4 km southeast of S. Venerina. Contemporaneously, the nearby Timpe Fault System (Fig. 1) was reactivated, with displacements of several centimeters. On 26 November, a shallow Md 2.6 earthquake along the Trecastagni Fault (Fig. 1) was followed by ground fracturing near Trecastagni, with a N120° dextral transpressive movement and 0.02–0.04 m of displacement. Movement of the eastern flank of the volcano was thus confined between the PFS to the north and the Trecastagni fault to the SE. No surface evidence for movement was recorded at the Ragalna fault system during the period of the eruption.

Deformation pattern along the PFS and its new easternmost extent

During the 2002–2003 sequence of events the initial deformation on the PFS was in its westernmost portion, immediately after the 22 September earthquake. This consisted of surface fractures with a left-lateral displacement of 0.48 m (Table 1). At the end of October, contemporaneously with the opening of the NE Rift eruptive fissures, the westernmost PFS (Fig. 4) became active again, with an almost purely left-lateral displacement of ~ 0.7 m. The total displacement since 22 September measured in this portion on 12 November exceeded 1.25 m at 1,450 m a.s.l. (Fig. 5). Further to the E, the PFS moved with a decreasing left-lateral displacement, reaching 0.38 m at 790 m a.s.l. (Fig. 6; Table 1). Near Presa (Fig. 7) the deformation was transferred into several subparallel E–W-trending segments with a dextral en-echelon configuration and left-lateral kinematics; furthermore these segments were linked by more or less N–S-trending thrust faults (due to their small extent they

Table 1 Main structural features of the PFS associated with the 2002–2003 Etna eruption. total slip rates calculated along the PFS are obtained by summing up the slip rates calculated. The data has been collected along man-made features, such as roads, walls and buildings. The before September 2002 and those relative to the 2002–2003 eruption

| n° | Location | Figure | Structure | Altitude a.s.l. (m) | Coordinates | | | Geometric parameters | | | 2002 eruption displacement | | | | | Progression of the horizontal displacement during the 2002 eruption (m) | | | | | Total displac. before 2002 eruption (m) | | Displaced object | Slip rates | | Reference | |
|----|------------------|--------|-----------|---------------------|-------------|------------|------------|----------------------|---------|------------|----------------------------|----------------|----------------------|------------|--------|---|--------|--------|--------|--------------------------|---|-----------------------------|-------------------|--|-----------------------------|-------------------------------|--|
| | | | | | Lat N | Long E | Strike (°) | Dip dir. (°) | Dip (°) | Length (m) | Vertical (m) | Horizontal (m) | Calculated pitch (°) | Kinematics | 22 Sep | 27 Oct | 12 Nov | 20 Nov | 22 Dec | Vertical (m) | Kinematics | Before Sept. 2002 (cm/year) | | Total at 22/12/2002 (cm/year) | | | |
| 1 | 2002 fissure | 4 | Def | 1,870 | 37,80628° | 15,04022° | 80 | 170 | 90 | 17,220 | >1 | >2 | 125 | LLT | 0 | >2 | >2 | >2 | >2 | >2 | Left-lateral transensive | 0 | >2 | Present-day apron | Before Sept. 2002 (cm/year) | Total at 22/12/2002 (cm/year) | This paper |
| 2 | Provenzana | 4 | PFs | 1,816 | 37,800759° | 15,03656° | 65 | 155 | 80 | 3,500 | 0.05 | >1 | 90 | LLT | 0.03 | >1 | >1 | >1 | >1 | >1 | Left-lateral transensive | 0 | >1 | 1986 A.D. roads and buildings | 2.2±0.1 | | This paper |
| 3 | Vill. Mareneve | 4 | PFs | 1,450 | 37,808801° | 15,069796° | 90 | 180 | 85 | 17,220 | 0.6 | >1.25 | 100 | LLT | 0.48 | 1.10 | >1.25 | >1.25 | >1.25 | >1.25 | Left-lateral transensive | 0.6 | 0.6 | 1980 A.D. road and concrete wall | 1.6±0.1 | 2.2±0.1 | This paper and Tibaldi and Gropelli (2002) |
| 4 | Mandra del Re | 4 | PFs | 1,130 | 37,80748° | 15,09915° | 95 | 185 | 85 | 17,220 | >0.1 | >0.4 | 125 | LLT | 0 | >0.4 | >0.4 | >0.4 | >0.4 | Left-lateral transensive | 0 | >0.4 | Present-day apron | 1.5 | 2.3 | This paper | |
| 5 | Rocca Pignatello | 7 | PFs | 850 | 37,80176° | 15,12836° | 100 | 190 | 85 | 17,220 | 0 | 0.18 | 130 | LL | 0 | 0.10 | 0.18 | 0.18 | 0.18 | 0 | Left-lateral | 0 | 0 | 1840±10 A.D. neglected cart track | 2.2±0.1 | | Rasà et al. (1996) |
| 6 | Rocca Campana | 7 | PFs | 790 | 37,80112° | 15,13336° | 95 | 185 | 85 | 17,220 | 0 | 0.40 | 135 | LL | 0.01 | 0.12 | 0.38 | 0.38 | 0.40 | 0 | Left-lateral | 0 | 0 | 1940±3 A.D. road SP 59 and stone wall | 1.4±0.1 | 1.4±0.1 | This paper and Tibaldi and Gropelli (2002) |
| 7 | Rocca Campana | 7 | PFs | 780 | 37,80100° | 15,13631° | 92 | 182 | 85 | 17,220 | 0 | 0.26 | 135 | LL | 0 | 0.10 | 0.26 | 0.26 | 0.26 | 0 | Left-lateral | 0 | 0 | 1972 concrete wall and building | 0.8±0.2 | 1.4±0.3 | This paper |
| 8 | Rocca Campana | 7 | PFs | 780 | 37,79963° | 15,13328° | 92 | 182 | 85 | 17,220 | 0 | 0.18 | 130 | LL | 0 | 0.10 | 0.18 | 0.18 | 0.18 | 0 | Left-lateral | 0 | 0 | 1940±3 A.D. road SP 59 and stone wall | 0.9 | 1.0 | This paper |
| 9 | Vena-Presa | 7 | PFs | 680 | 37,79487° | 15,14378° | 100 | 190 | 85 | 17,220 | 0.1 | 0.39 | 110 | LLT | 0 | 0.07 | 0.35 | 0.35 | 0.39 | 0 | Left-lateral | 0 | 0 | 1940±10 A.D. road SP 68 and stone wall | 1.8±0.3 | 2.3±0.4 | This paper |
| 10 | Presa | 7 | PFs | 580 | 37,79339° | 15,14722° | 180 | 270 | 40 | 60 | 0.07 | 0.18 | 90 | C | 0 | 0.09 | 0.18 | 0.18 | 0.18 | 0 | Compressive | 0 | 0 | Concrete wall and iron fence | 1.8±0.3 | 2.3±0.4 | This paper |
| 11 | Presa | 7 | PFs | 580 | 37,79341° | 15,14736° | 90 | 180 | 85 | 17,220 | 0 | 0.175 | 110 | LL | 0 | 0.02 | 0.175 | 0.175 | 0.175 | 0 | Left-lateral | 0 | 0 | 1965±5 A.D. Montargano-Presa road and stone wall | 0.8±0.2 | 1.4±0.3 | This paper and Tibaldi and Gropelli (2002) |
| 12 | Presa | 7 | PFs | 575 | 37,79334° | 15,147959° | 180 | 270 | 40 | 35 | 0.09 | 0.26 | 90 | C | 0 | 0.26 | 0.26 | 0.26 | 0.26 | 0 | Compressive | 0 | 0 | Concrete wall | 1.8±0.3 | 2.3±0.4 | This paper |
| 13 | S. Venera | 7 | PFs | 218 | 37,78237° | 15,17235° | 85 | 175 | 85 | 17,220 | 0 | 0.05 | 150 | LL | 0 | 0.05 | 0.05 | 0.05 | 0.05 | 0 | Left-lateral | 0 | 0 | Stone wall and SP2 road | 0.9 | 1.0 | This paper |
| 14 | S. Venera | 7 | PFs | 160 | 37,782216° | 15,178790° | 70 | 160 | 85 | 17,220 | 0.01 | 0.025 | 90 | LLT | 0 | 0.025 | 0.025 | 0.025 | 0.025 | 0 | Left-lateral | 0 | 0 | SP67 road | 0.9 | 1.0 | This paper |
| 15 | A18 Highway | 7 | PFs | 121 | 37,779804° | 15,184925° | 95 | 185 | 85 | 17,220 | 0.02 | 0.05 | 110 | LLT | 0 | 0.03 | 0.03 | 0.03 | 0.05 | 0 | Left-lateral | 0 | 0 | Concrete borders of the A18 Highway CT-ME | 1.8±0.7 | 1.9±0.7 | This paper |
| 16 | Gona | 7 | PFs | 55 | 37,774191° | 15,198236° | 105 | 195 | 85 | 17,220 | 0 | 0.08 | 116 | LL | 0 | 0.06 | 0.06 | 0.08 | 0 | 0 | Left-lateral | 0 | 0 | 1930±20 A.D. stone walls and SPI road | 1.8±0.7 | 1.9±0.7 | This paper |
| 17 | Fon-dichello | 7 | PFs | 5 | 37,772145° | 15,225077° | 55 | 145 | 85 | 17,220 | 0.01 | 0.02 | 118 | LLT | 0 | 0.02 | 0.02 | 0.02 | 0.02 | 0 | Left-lateral | 0 | 0 | Riposto-Schiso road | 1.8±0.7 | 1.9±0.7 | This paper |

def 2002 dry and eruptive fissure; PFs Pernicana Fault system; LL left-lateral; LLT left-lateral transensive; C compressive

Fig. 4 Structural map of the western portion of the PFS during the 2002–2003 eruption (as observed in mid-November 2002) and the NE Rift

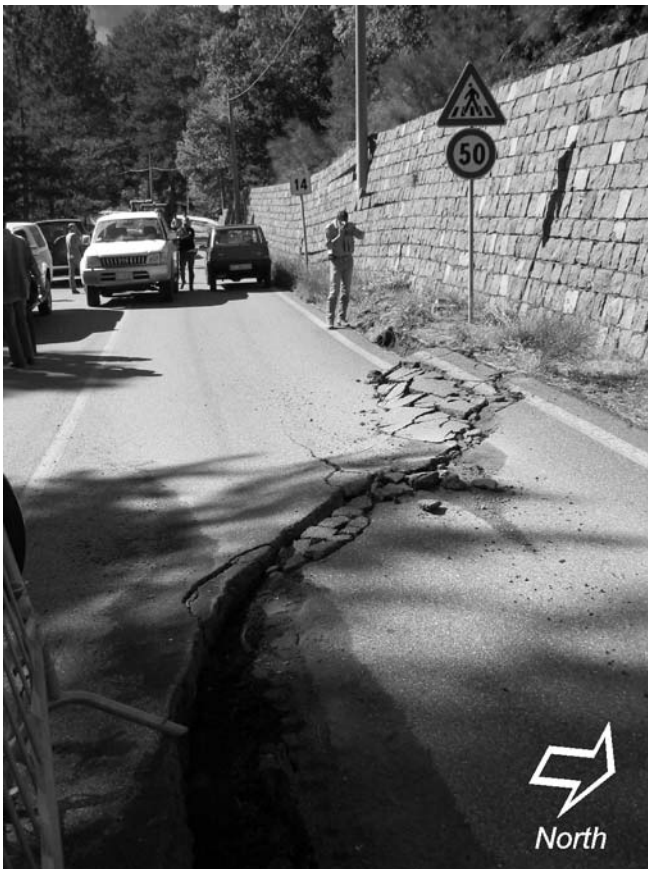
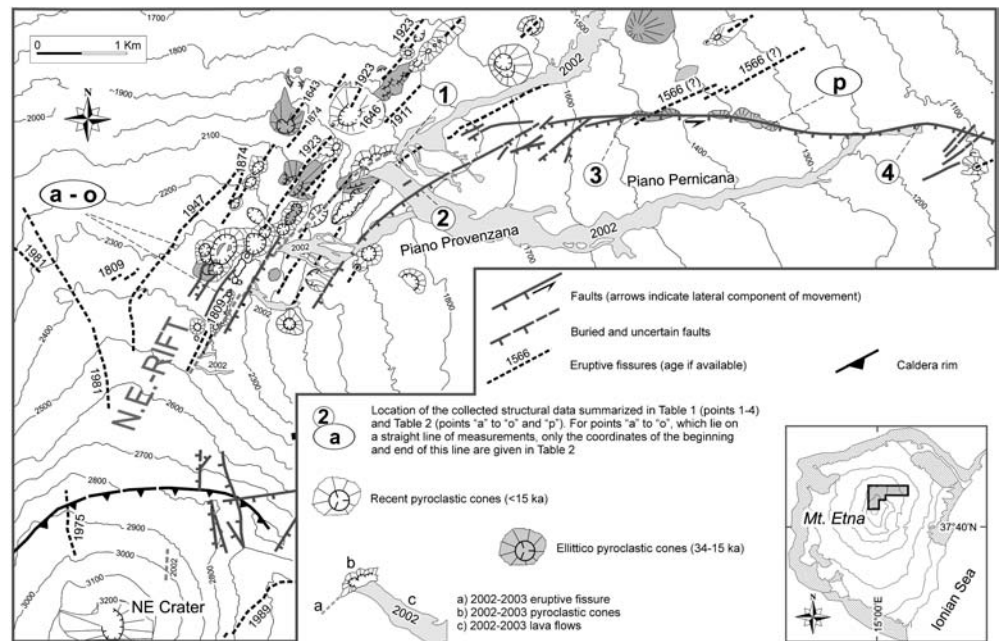


Fig. 5 Fractured S.P. Mareneve Nord road (see Fig. 2 and point 3 in Fig. 4 for location) on the westernmost portion of the PFS, on 12 November 2002. Total horizontal displacement of the fractures is >1.25 m, with a vertical component of ~0.5 m. Note vertical displacement of stone wall in right background; extensimeters mentioned in the text (see also Fig. 3) were installed on rear side of this wall in 1994

do not appear in Fig. 7). These thrust faults might correspond to the more shallow of the two detachment surfaces proposed by Tibaldi and Groppelli (2002) to cut the surface near Presa. The overall deformation pattern, as visible around mid-November along the western PFS and the relationships between the PFS and the NE Rift are shown in Fig. 4.

After 29 October, fracturing propagated further eastward, towards the Ionian coast, beyond the termination of the formerly known PFS. Here, deformation was evident on paved roads and showed an overall WNW–ESE trend; the trace of this eastern portion of the PFS is shown in Fig. 7 (to distinguish the previously known western portion of the PFS from its previously unknown eastern continuation, we term them “western PFS” and “eastern PFS”, respectively). The eastern PFS thus continued in the form of regularly spaced N80°E-trending fault segments with a dextral en-echelon configuration, both on a large and a small scale (Figs. 8 and 9). These faults were mainly characterized by a left-lateral shear, with minor normal displacement; the mean horizontal displacement along single segments decreases from 0.08 (Gona) to 0.02 m at the coastline (Table 1).

An important feature of the eastern PFS is that it coincides with man-made structures, which have been previously displaced and partly repaired in the past few decades. Along this fault zone, it is in fact possible to distinguish the 2002 displacement from previous movement. As an example, Fig. 9 shows a paved road displaced by the eastern PFS, near the village of Gona (Figs. 7 and 9). Here, the 2002 left-lateral displacement (visible on the white median strip of a road) reaches 0.08 m, but the 2002 fault zone is located in correspondence with a pre-existing ruptured wall, which shows a left-lateral displacement of 1.37 m in the last ~70 years (the age of the wall). This

Fig. 6 Evolution of the horizontal displacement along a fault splay cutting across a road in the central PFS at Rocca Campana, near the village of Presa (see point 6 in Fig. 7). The overall left lateral shear (0.38 m on 12 November 2002) is clearly visible at the displaced white median strip

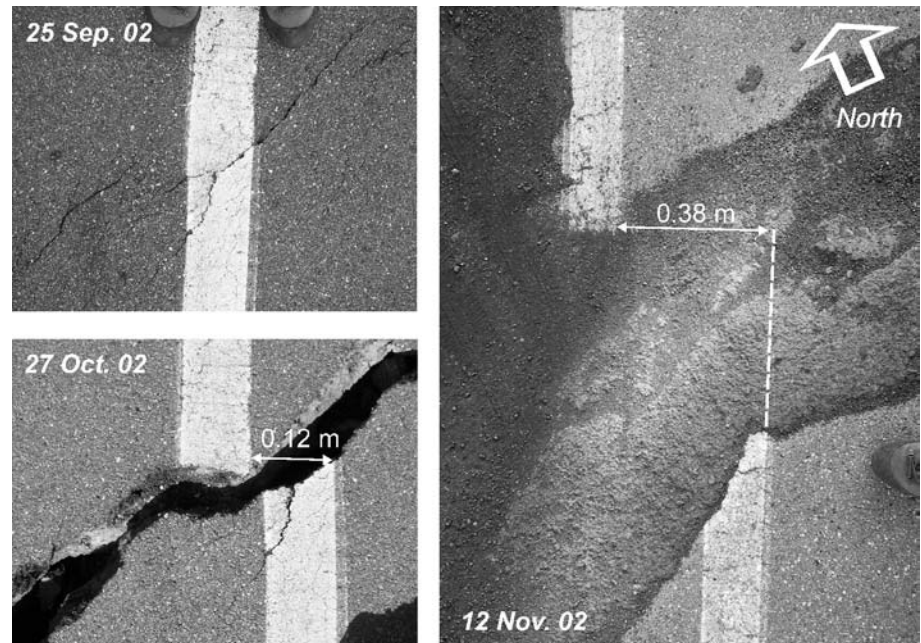
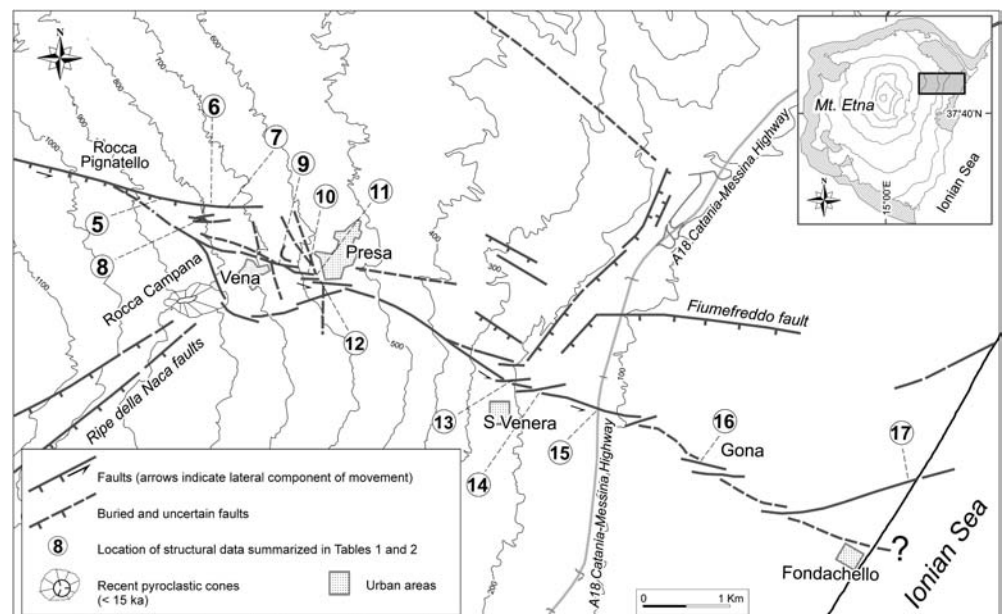


Fig. 7 Structural map of the eastern, mostly (between Presa and Fondachello) newly activated and previously unknown, portion of the PFS developed during the 2002–2003 eruption (as observed in mid-November 2002)



indicates that the 2002 fractures which constitute the eastern PFS reactivated this structure, which has probably been creeping in the past decades. The full, uninterrupted, and measurable on-shore length of the PFS is therefore nearly 18 km (Figs. 4 and 7).

As noted above, movement beyond the eastern termination (as known until the 2002–2003 eruption) of the PFS was previously believed to be transferred along the Fiumefreddo Fault (Fig. 7) (Azzaro et al. 1998; Tibaldi and Groppelli 2002), lying a few kilometers to the north of the newly ruptured eastern PFS. However, during the 2002 events, the Fiumefreddo Fault remained locked and inactive.

Long and short term slip-rates along the PFS

The PFS has been studied for many years and has left evident traces of activity in geological features (lava flows and pyroclastic cones) as well as in man-made structures (roads, walls, buildings, etc.). The activity on both man-made and geological features is briefly summarized in Tables 1 and 2, respectively, which quantify the style of deformation of the entire NE sector of the volcano, including the NE Rift and the full length of the PFS.

Overall extension along the NE Rift is oriented N117° and occurred at an average rate of 2.6 ± 0.5 cm/year for at

Table 2 Main structural features of the PFS associated with the 2002–2003 Etna eruption, PFS (p in Fig. 7) give a similar value, ~ 2.65 cm/year. Measurements were made on a as observed from the displacement of geological features, or, partly, from previous works. straight line (see coordinates of western and eastern extremities of this line) perpendicular The mean slip rates calculated for the NE Rift (a-o in Fig. 7) and the western portion of the to the trend of the NE Rift

| Station of measure | | Coordinates | | | Geometric parameters | | | | Kinematics | | Displaced geological unit | | Slip rate | | Reference | | | |
|--------------------|--------------------|-------------|-------------|---------------------|----------------------|-----------|------------|--------------|------------|------------|---------------------------|-------------|-----------|--------------|-----------------------|----------------------------------|---------------------|--------------------------------------|
| n° | Location | Fig-ure | Struc- ture | Altitude a.s.l. (m) | Lat N | Long E | Strike (°) | Dip dir. (°) | Dip (°) | Length (m) | Apert. (m) | Upthrow (m) | Heave (m) | Kine- matics | Calcu- lat. Pitch (°) | Displaced geological unit | Slip rate (cm/year) | Reference |
| a | NE Rift | 4 | Def | 2,400 | 37,79274° | 15,01397° | 41 | 131 | 85 | 1,800.5 | 3 | 3 | 0 | N | 90 | 1874 A.D. lava flows | 2.6±0.5 | This paper and Garduño et al. (1997) |
| b | NE Rift | 4 | Def | 2,413 | | | 25 | 295 | 85 | 150 | 0.45 | 1.5 | 0.08 | LLT | 87 | 1923 A.D. cones | | This paper and Garduño et al. (1997) |
| c | NE Rift | 4 | Def | 2,390 | | | 22 | 112 | 85 | 100 | 0.2 | 0.15 | 0.05 | LLT | 72 | 1614–64 A.D. lava flows | | This paper and Garduño et al. (1997) |
| d | NE Rift | 4 | Def | 2,390 | | | 20 | 290 | 90 | 100 | 0.3 | 0.05 | 0.05 | LLT | 45 | 1614–64 A.D. lava flows | | This paper and Garduño et al. (1997) |
| e | NE Rift | 4 | Def | 2,390 | | | 10 | 100 | 90 | 100 | 0.18 | 0 | 0 | N | ~ | 1614–64 A.D. lava flows | | This paper and Garduño et al. (1997) |
| f | NE Rift | 4 | Def | 2,390 | | | 19 | 109 | 90 | 100 | 0.15 | 0 | 0.07 | LLT | 0 | 1614–64 A.D. lava flows | | This paper and Garduño et al. (1997) |
| g | NE Rift | 4 | Def | 2,390 | | | 0 | 270 | 90 | 100 | 0.8 | 0.09 | 0.07 | RLT | 52 | 1614–64 A.D. lava flows | | This paper and Garduño et al. (1997) |
| h | NE Rift | 4 | Def | 2,390 | | | 20 | 290 | 90 | 200 | 0.8 | 0.15 | 0.09 | RLT | 59 | 1614–64 A.D. lava flows | | This paper and Garduño et al. (1997) |
| i | NE Rift | 4 | Def | 2,390 | | | 10 | 100 | 90 | 300 | 0.08 | 0 | 0.04 | RLT | 0 | 1614–64 A.D. lava flows | | This paper and Garduño et al. (1997) |
| j | NE Rift | 4 | Def | 2,390 | | | 9 | 279 | 90 | 350 | 0.14 | 0.09 | 0 | N | 90 | 1614–64 A.D. lava flows | | This paper and Garduño et al. (1997) |
| k | NE Rift | 4 | Def | 2,390 | | | 12 | 102 | 90 | 300 | 0.5 | 0.3 | 0.07 | RLT | 77 | 1614–64 A.D. lava flows | | This paper and Garduño et al. (1997) |
| l | NE Rift | 4 | Def | 2,345 | | | 20 | 110 | 85 | 180 | 3 | 0.07 | 0.6 | LLT | 85 | 1923 A.D. cone | | This paper and Garduño et al. (1997) |
| m | NE Rift | 4 | Def | 2,093 | | | 26 | 116 | 85 | 140 | 0 | 1.5 | 0 | N | 90 | Recent lava flows | | This paper and Garduño et al. (1997) |
| n | NE Rift | 4 | Def | 2,093 | | | 26 | 116 | 85 | 140 | 0 | 1.5 | 0 | N | 90 | Recent lava flows | | This paper and Garduño et al. (1997) |
| o | NE Rift | 4 | Def | 2,400 | 37,79715° | 15,00766° | 30 | 300 | 85 | 1,700 | 1.5 | 1.5 | 0 | N | 90 | 1614–64 A.D. lava flows | | This paper and Garduño et al. (1997) |
| p | Villaggio Mareneve | 4 | PFS | 1,370 | 37,8077° | 15,07982° | 100 | 190 | 80 | 17,220 | 50±10 | 370±20 | LLT | LLT | 130 | Pyroclastic cone 13700±2400 B.P. | 2.7±0.7 | Tibaldi and Groppelli (2002) |

def Dry and eruptive fissure; *PFs* Pemicana Fault system; *N* normal; *LL* left-lateral; *LLT* left-lateral transpressive; *RLT* right-lateral transpressive; *C* compressive

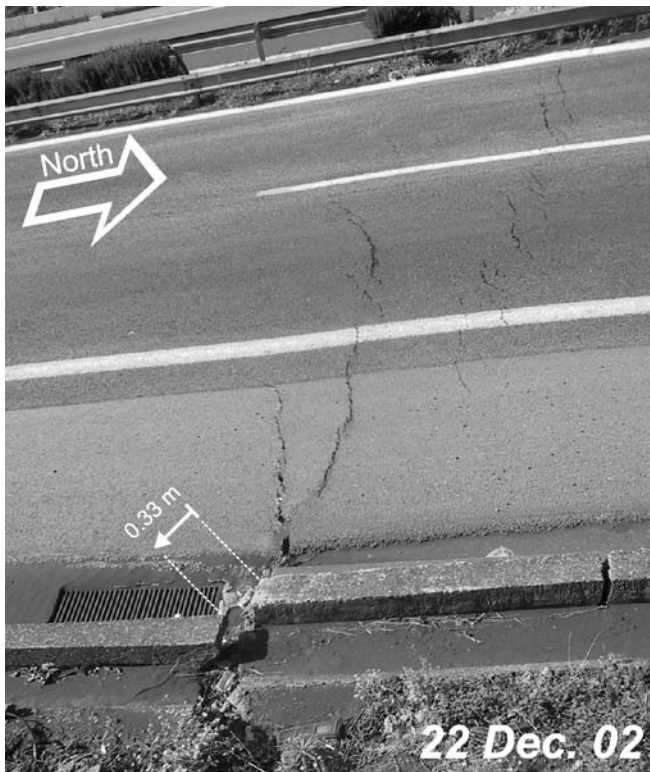
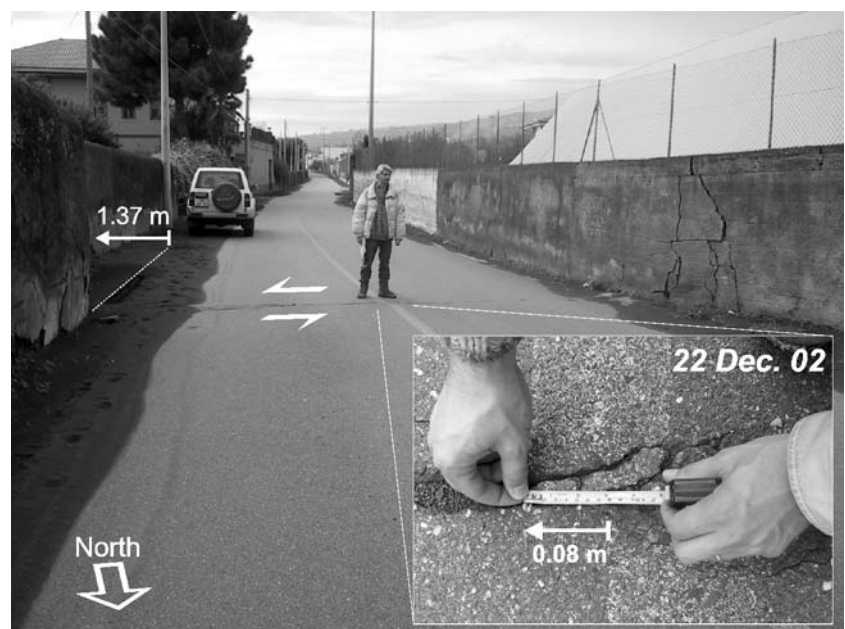


Fig. 8 Typical deformation pattern of the eastern PFS, across the surface of the A18 Catania-Messina Highway (point 15 in Fig. 7). Deformation is characterized by a set of ~E-W-trending en-echelon fractures, arranged in a dextral configuration, with a predominant left-lateral shear and a subordinate extensional component. At the border of the highway, 0.33 m (of which 0.05 m is related to movement through 22 December 2002 and 0.28 m is due to previous episodes since 1971, when the highway was constructed) of horizontal displacement is marked by the shift of the small concrete wall in the foreground

Fig. 9 Paved road displaced by the newly formed eastern PFS, near Gona (see Fig. 7 for location). Here the 2002 fault zone shows left-lateral displacement (of the white median strip) by 0.08 m (as observed on 22 December 2002). However, the fault zone is located in correspondence with a previously unknown fault, which displaced the walls on both sides of the road in the last ~70 years (left-lateral displacement of 1.37 m)



least 400 years prior to 2002. Similar values, 2.7 ± 0.7 cm/year, are obtained from the observed displacement of two portions of a prehistoric (13.7 ± 2.4 ka) pyroclastic cone dissected by the western PFS (Tibaldi and Groppelli 2002).

Man-made structures, even though representative of a much shorter time period, provide important information about the more recent deformation. With this regard, Table 1 shows the slip rates obtained from man-made structures and the displacements observed during the 2002–2003 eruption (at different intervals) along the entire PFS. In particular, Table 1 shows that the estimated post-1930 slip rates for the entire PFS (excluding the 2002–2003 data) range from 0.8 ± 0.2 to 2.2 ± 0.1 cm/year; there is a general tendency in the decrease of the slip rates towards east. If, on the other hand, we include the displacements observed during the 2002–2003 eruption (keeping the time span constant), we obtain total rates that range from 1.0 to 2.3 ± 0.4 cm/year. These values are indeed closer to the longer-term values obtained from the geological features in Table 2.

The portion of the PFS with the largest displacement during the 2002–2003 eruption is its western part, between the NE Rift and Presa; here the horizontal displacement ranges from 1.25 m (Villaggio Mareneve, Table 1) to 0.26 m (Presa, Table 1). Conversely, the measured displacement along the eastern PFS is between 0.08 and 0.05 m. From the observed horizontal displacements, a daily slip rate of ~0.015 m (between September and November) can be estimated for the western PFS, while in the eastern PFS the slip rate is lower by more than one order of magnitude (Table 1).

Nearly daily measurements of surface deformation along the PFS revealed that its various portions moved quite differentially. Table 1 shows that the western PFS was mostly active between the 22 September earthquake

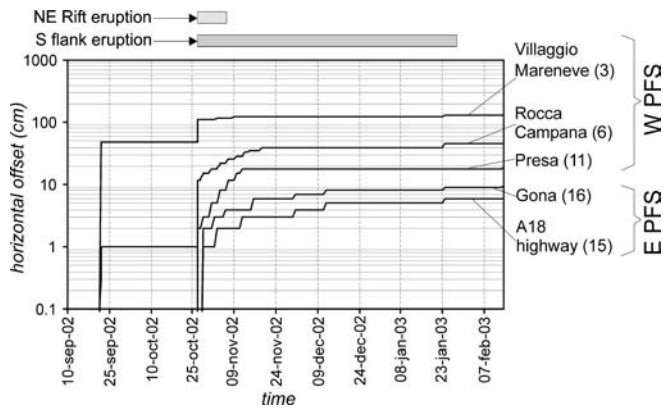


Fig. 10 Variation of the left-lateral displacement with time along portions of the PFS

and the beginning of November; conversely, activity at the eastern PFS was focused between the end of October and the beginning of November. Some portions of the central (Vena-Presa area in Table 1) and the eastern (Highway and Gona in Table 1) PFS remain active at the time of writing (June 2003). The timing of the left-lateral displacement along selected portions of the PFS (see Table 1 for their locations) is shown in Fig. 10. It thus appears that the deformation propagated from west to east: it started from the NE Rift area and then migrated to the eastern PFS; after early November, the western portion became temporarily locked, with slight activity continuing in the central and eastern portion, through late-February 2003. Renewed fault slip accompanied by shallow seismicity occurred at the western PFS on 13–14 February 2003.

Discussion

The new extent of the PFS and its features in the context of the 2002–2003 eruption

The 2002–2003 Etna eruption and the related deformation have provided a unique occasion to recognize the previously unknown on-land extent of the Pernicana Fault System, from the NE Rift to the coastline; at present we do not have the necessary data to define the features and extent of its off-shore continuation. On land, the PFS is nearly 18 km long and is characterized by consistent kinematics, given by a predominant left-lateral and a subordinate extensional component of motion. Despite its continuity, the PFS can be roughly divided into two main portions (western and eastern), characterized by differential times and amounts of displacement. The western PFS, ~9 km long (from the NE Rift to Presa), coincides with the previously known portion of the fault. During the 2002–2003 eruption this was characterized by larger (at least by one order of magnitude) displacements compared to those of the eastern PFS, even though the long-term slip rates are similar in both portions of the PFS (Tables 1

and 2). Moreover, the western PFS is associated with shallow seismic activity (e.g. the 22 September 2002 earthquake), which is lacking along the eastern PFS. The eastern PFS, ~9 km long (from Presa to the coastline), is the newly activated aseismic portion recognized during the 2002–2003 eruption. This portion is located on a previously active but unknown fault zone with no recorded historical seismicity.

The different deformation styles of the western and eastern PFS may be partly related to the different physical properties of their substratum. There is a thick pile of lava flows in the western sector and in the eastern sector a thin (locally even absent) volcanic cover overlying plastically deformable marly-sands and clay sediments. As a consequence, the higher compressibility of the more ductile sediments to the east might be able to accommodate and broaden the deformation, resulting in a more limited surface expression. In contrast, the lava flows in the western and central portion of the PFS are brittle and very elevated susceptibility to fracturing, and thus strongly focus any ground movement.

The 2002–2003 eruption and ground deformation furthermore show that the Fiumefreddo Fault is probably not, as previously thought (Lo Giudice and Rasà 1992; Azzaro et al. 1998; Tibaldi and Groppelli 2002), the main eastern continuation of the PFS. The Fiumefreddo Fault remained locked during the 2002–2003 eruption and the PFS propagated eastward, a few kilometers further to the south, along a previously active but unknown structure. While we cannot fully exclude some kind of genetic relationship between the PFS and the Fiumefreddo Fault, the field geometries (Fig. 7) and the lack of any movement at the latter fault during the major 2002–2003 slip event implies that its association with the PFS is at best marginal. Evaluation of the exact location of the active structures along the NE flank of Etna and their availability for mobilization during an eruption is of crucial importance because of the presence of villages and major communication lines, such as the Catania-Messina highway and the State Railroad (Fig. 7), all of which lie in the area affected by the 2002–2003 ground deformation.

The 2002–2003 eruption has also allowed to further test the kinematic connection between the NE-Rift and the PFS. In fact, a feedback process between the opening of the NE Rift and the eastward sliding (along the PFS) of Etna's flank has been proposed previously (Neri et al. 1991; Garduño et al. 1997; Tibaldi and Groppelli 2002; Acocella and Neri 2003). During the event discussed here, such a feedback was marked by (1) the 22 September earthquake and associated surface rupture along the western PFS (2) the eruption along the NE Rift five weeks later, and (3) the subsequent activation of the whole PFS (Fig. 11).

The fact that magma rose within the central conduit system and then propagated laterally into the NE Rift, rather than ascending vertically directly beneath it, implies that the 22 September earthquake was not induced by shallow (intra-edifice) magma movement. Instead, this suggests that the earthquake was caused by gravitational

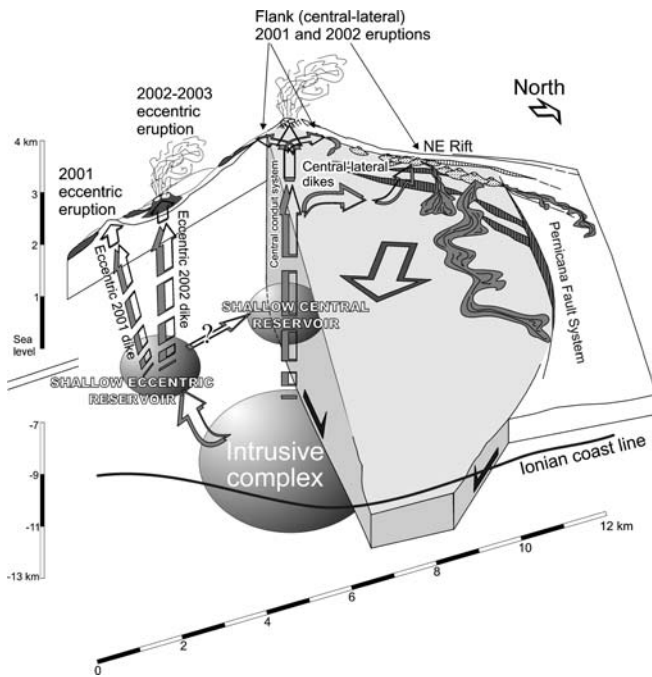


Fig. 11 Proposed model of spreading on the eastern flank of Etna. Slippage occurs by means of a feedback process between volcanic activity (mainly from the NE Rift) and gravitational instability of the flank, bordered to the north by the PFS. The spreading area is possibly confined to a depth of ~4 km b.s.l., where a deep décollement is inferred. Approximate scale is shown

instability on the eastern flank of the volcano, possibly enhanced by sub-volcanic magma accumulation and inflation (Patanè et al. 2003). The instability unlocked the rift after 55 years of quiescence and thus served as a primary trigger for the eruption there. The earthquake was indeed immediately followed by a rapid withdrawal of the magma that had been present until then within the NE Crater. The eastward movement related to the 22 September earthquake (as well as the similar shallow earthquakes on 26 October) may have led to a localized decompression in the NE Rift area, hereby facilitating the extrusion of magma. In this context, the magma emission on the NE flank can be interpreted as a passive eruption, which drained most of the central conduit system and ended once this (relatively limited) storage area was exhausted. The simultaneous eruption from the fissure on the S flank (F1) may also have been somehow triggered by these events; nevertheless, its prolonged duration indicates constant supply from a shallow reservoir that is independent from the central conduit system (Fig. 11).

Implications for flank spreading at Etna

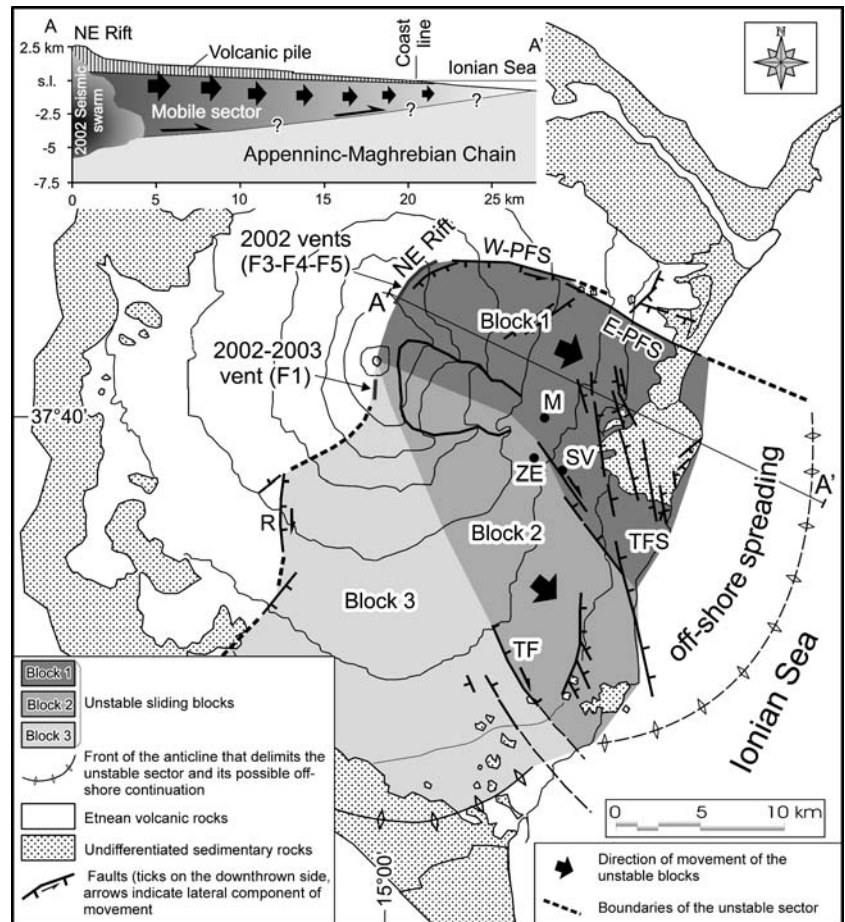
The opening of the NE Rift during the 2002–2003 eruption resulted in the activation of the whole PFS. The close association of the eruptive and deformative events, the eastward decrease of displacement along the PFS and the successive activation of its eastern segment suggest

that the opening of the NE Rift triggered the eastward displacement on the eastern flank of the volcano. The area thus mobilized extends from the NE-Rift to somewhere beneath the Ionian Sea (Fig. 12).

Surface deformation migrated then southwards, reaching, at the beginning of November, the Timpe Fault System and, at the end of November, the Trecastagni Fault (Fig. 2). Until late February 2003, no reactivation has been observed along the Ragalna Fault, which is believed to be the western boundary of the southern portion of the spreading area at Etna (Fig. 2) (Rust and Neri 1996). This indicates that, so far, the displacement is limited to the E part of the volcano. It did not occur in a single, instantaneous event, but showed a progression first from west to east along the PFS and then from north (slide block 1 between the PFS and S. Venerina) to south (slide block 2 between S. Venerina and Trecastagni) (Fig. 12). We assume that the clustering of the late-October shallow earthquakes along a NW-SE direction, from Zafferana to Acireale, marks the southern boundary of slide block 1. Part of this area was also affected by fracturing and anomalous radon emission before and during the initial phase of the 2002–2003 eruption. Moderate ground fracturing at Trecastagni marked, with dextral shear, the southern border of slide block 2. Further movement of this block cannot be excluded in the near future and might even be followed by the activation of the (thus far inactive) southernmost portion of Etna's unstable sector, between the Trecastagni and Ragalna Faults (slide block 3 in Fig. 12).

The observed sequence of events permit us to precisely establish the timing of the various stages of displacement. Movement started along the western PFS, before the eruption, probably as a consequence of gravitational instability, which, in turn, might have been enhanced by the resumption of magma accumulation below the volcano. The eruption-related rifting (i.e. the largely passive intrusion of a dike) then led to the activation of the whole PFS, including its previously unknown eastern portion. Soon after the entire PFS had become activated, the western PFS became temporarily locked, while the central and eastern sectors were still characterized by a slow but persistent activity that occurred in a creep-like manner. This suggests a peculiar mode of propagation of the deformation during the flank slip, which is in fact characterized by deformation extending from higher towards lower elevations, with a less pronounced but prolonged activity in the more distal areas. The locking of the western PFS and the more long-lived creeping along the central-eastern PFS may be the result of the different physical properties and behavior of the substratum (lavas vs. clays) below the two respective portions. In fact, the prolonged movement of the eastern PFS might in part be related to the propagation of a pressure wave across the viscous sub-volcanic clay sediments. During the 2002–2003 eruption, the displacements along the PFS showed an eastward decrease by more than one order of magnitude. We believe that, over much longer time spans (tens to thousands of years) as compared to the duration of

Fig. 12 Sketch map of Mt. Etna, showing its unstable eastern flank, affected by differential movement during the 2002–2003 eruption. *Inset* at upper left shows a hypothetical NW–SE section through sliding block 1, parallel to its direction of movement. *W-PSF* western PFS; *E-PFS* Eastern PFS; *M* Milo; *SV* Santa Venerina; *ZE* Zafferana Etnea; *TF* Trecastagni Fault; *TFS* Timpe Fault System; *R* Ragalna Faults. The front of the anticline that delimits the unstable sector is modified from Borgia et al. (2000b)



an eruption, creeping of the eastern PFS is able to achieve the same long-term slip-rates as the western PFS (Table 1).

The newly traced PFS, from the NE Rift to the coastline, also yields insights on the extent and volume of the spreading flank of the volcano. Field evidence indicates that the mobile area on the eastern flank of Etna reaches the Ionian Sea. Different depths (between 2 km a.s.l. to 6 km b.s.l.) have been proposed for the décollement below the eastern flank of Etna (Kieffer 1985; Lo Giudice and Rasà 1992; Borgia et al. 1992; Bousquet and Lanzafame 2001). Focal depths of the earthquakes on the eastern flank of the volcano during the 2002 slip event, distant from the magmatic conduits and therefore not related to magma movement, may be taken as an indicator for the thickness of the sliding mass. The hypocenters of most of these earthquakes cluster above ~4 km b.s.l., with little evidence of deeper seismicity (Patanè 2002). If we consider these earthquakes as an expression of the deep readjustment of the 2002 slip event, we obtain a depth of ~4 km b.s.l. for the basal décollement at Etna. This depth is close to the deep-seated décollement proposed by Borgia et al. (1992) to be related to the intrusion of magma within a plutonic complex beneath the volcano.

Table 3 Approximate volumes of the slide blocks on the eastern and southern flanks of Etna, calculated considering only their on-shore extent (minimum estimate, Fig. 12) and the possible décollement depth for the onshore area (minimum estimate), inferred from the distribution of seismicity. Slide blocks 1 and 2 involve a minimum volume of 1,100 km³ of rock

| | Average thickness (km) | Area (km ²) | Volume (km ³) |
|---------|------------------------|-------------------------|---------------------------|
| Block 1 | 3 | 210 | 630 |
| Block 2 | 3 | 157 | 471 |
| Block 3 | ? | 337 | ? |
| Total | | 704 | 1101 |

We believe that the shallower detachment surface proposed by Tibaldi and Groppelli (2002), which is considered by these authors to cut the topography in the ~N–S-trending thrust faults near the village of Presa (Fig. 7), might well exist, but in the context of the 2002–2003 slip merely represents a second-order structural element.

Surface data (such as the extent of the fractured area) and subsurface data (the distribution of the seismicity) permit a rough evaluation of the volume of the moving mass on the eastern flank of Etna (Table 3). At surface, slide block 1 has an on-shore extent of ~210 km², while slide block 2 has an on-shore extent of ~157 km²

(Fig. 12). At depth, the seismicity below the eastern flank suggests a décollement at ~4 km b.s.l. If we assume, for a safe estimate, that the décollement rises from ~4 km b.s.l. below the NE Rift to sea level at the coastline, the mean thickness of the sliding mass is 3 km, of which ~2 km lie below sea level and ~1 km above sea level (Fig. 12). This gives an overall volume of ~1,100 km³ of material moving towards the Ionian Sea. This volume has to be considered a minimum estimate, as it does not take into account any possible offshore continuation of the area affected by slippage. The total volume mobilized during the 2002–2003 eruption thus corresponds to about three times the volume of the volcanic pile of Etna (Neri and Rossi 2002), and by far the greatest proportion of rock incorporated in the slide is represented by the sedimentary substratum.

Conclusions

Our observations during the 2002–2003 eruption of Mount Etna and the related slip of its unstable eastern to southeastern sector lead to the following results:

1. Movement of the Pernicana Fault System along its full 18 km length occurred in a differential manner, proceeding from fast but relatively short-lived displacement in its western portion to much slower movement in the eastern portion, which, however, extended over a much longer time period;
2. The eastern half of the Pernicana Fault System, poorly constrained until now, was for the first time surveyed in detail during a slip event;
3. Slippage of the unstable sector affected two slide blocks, the more northerly of which showed movement a few weeks before the more southerly began to move as well. Flank spreading at Mount Etna does thus not occur in a simple, wholesale manner, but instead consists of a precise sequence of distinct deformational events in space and time;
4. Throughout the 2002–2003 eruption, no field evidence for movement of the assumed third, southernmost slide block of Mount Etna was found, although the continued movement of the other two slide blocks might eventually be followed by an extension of the currently mobile sector on the third slide block;
5. Structural field data and instrumental seismic data permit to infer on the three-dimensional extent of the mobile sector and to roughly calculate its minimum volume at 1,100 km³, most of which is constituted by the sedimentary substratum of the volcano;
6. The 2002–2003 eruption, and in particular the activity on the NE Rift of Mount Etna, is interpreted to be a rather passive response to the flank slip, which in fact began five weeks prior to the eruption onset.

The available evidence indicates that the uprise of magma from an eccentric reservoir below the southern flank and the migration of magma from the central

conduit system into the NE Rift in 2002–2003 were but the latest stage in a process that possibly started with the sub-volcanic accumulation of magma, which, in turn, led to inflation and accelerated structural instability of the volcano. The major flank slip initiated in September 2002 occurred as a consequence of this instability and caused the rapid decompression of the plumbing system of the volcano, facilitating the uprise of magma to the surface. While this model is quite clear in the case of the 2002–2003 eruption, similar mechanisms might have acted during some of the previous flank eruptions of Etna, and our ongoing research is strongly focused in that direction.

Acknowledgements The authors wish to thank R. Funicello for his support during the research. This work was partly financed with GNDT funds co-ordinated by C. Faccenna at Roma Tre University. Benjamin van Wyk de Vries and Andrea Borgia are acknowledged for their constructive reviews which significantly improved the quality of the paper, along with the helpful additional comments by Associate Editor Raffaello Cioni.

References

- Acocella V, Neri M (2003) What makes flank eruptions? The 2001 Mount Etna eruption and its possible triggering mechanisms. *Bull Volcanol* 65:517–529 10.1007/s00445-003-0280-3
- Ando M (1979) The Hawaii earthquake of November 29, 1975: low dip angle faulting due to forceful injection of magma. *J Geophys Res* 84:7616–7626
- Azzaro R, Lo Giudice E, Rasà R (1988) Il terremoto di Piano Pernicana (Etna Nord) del 28/10/1988. Campo macrosismico e quadro deformativo fragile associato all'evento. *Boll GNV* 4:22–40
- Azzaro R, Branca S, Giammanco S, Gurrieri S, Rasà R, Valenza M (1998) New evidence for the form and extent of the Pernicana Fault System (Mt. Etna) from structural and soil-gas surveying. *J Volcanol Geotherm Res* 84:143–152
- Behncke B, Neri M (2003) The July–August 2001 eruption of Mount Etna (Sicily). *Bull Volcanol* 65:461–476 10.1007/s00445-003-0274-1
- Billi A, Acocella V, Funicello R, Giordano G, Lanzafame G, Neri M (2003) Mechanisms for ground-surface fracturing and incipient slope failure associated to the July–August 2001 eruption of Mt. Etna, Italy: analysis of ephemeral field data. *J Volcanol Geotherm Res* 122:281–294 10.1016/S0377-0273(02)00507-3
- Borgia A, Ferrari L, Pasquarè G (1992) Importance of gravitational spreading in the tectonic and volcanic evolution of Mt. Etna. *Nature* 357:231–235
- Borgia A, Delaney PT, Denlinger RP (2000a) Spreading volcanoes. *Ann Rev Earth Planet Sci* 28:539–570
- Borgia A, Lanari R, Sansosti E, Tesauro M, Berardino P, Fornaro G, Neri M, Murray JB (2000b) Actively growing anticlines beneath Catania from the distal motion of Mount Etna's décollement measured by SAR interferometry and GPS. *Geophys Res Lett* 27:3409–3412
- Bousquet JC, Lanzafame G (2001) Nouvelle interprétation des fractures des éruptions latérales de l'Etna: conséquences pour son cadre tectonique. *Bull Soc Géol Fr* 172:455–467
- Calvari S, Pinkerton H (2002) Instabilities in the summit region of Mount Etna during the 1999 eruption. *Bull Volcanol* 63:526–535
- Calvari S, INGV-CT scientific staff (2002) Update on the eruptive activity at Mt. Etna: Multidisciplinary evidence of magma refilling (abs). *Eos Trans. AGU* 83(47) Fall Meet, Suppl F1483

- Delaney PT, Denlinger RP, Lisowski M, Miklius A, Okubo PG, Okamura AT, Sako MK (1998) Volcanic spreading at Kilauea, 1976–1996. *J Geophys Res* 103:18003–18023
- Delaney PT, Denlinger RP (1999) Stabilization of volcanic flanks by dike intrusion: an example from Kilauea. *Bull Volcanol* 61:356–362
- Dvorak JJ, Okamura AT, English TT, Koyanagi RY, Nakata JS, Sako MK, Tanigawa WT, Yamashita WT (1986) Mechanical response of the south flank of Kilauea volcano, Hawaii, to intrusive events along the rift systems. *Tectonophysics* 124:193–209
- Ferrari L, Garduño VH, Neri M (1991) I dicchi della valle del Bove, Etna: un metodo per stimare le dilatazioni di un apparato vulcanico. *Mem Soc Geol Ital* 47:495–508
- Froger JL, Merle O, Briole P (2001) Active spreading and regional extension at Mount Etna imaged by SAR interferometry. *Earth Planet Sci Lett* 187:245–258
- Garduño VH, Neri M, Pasquarè G, Borgia A, Tibaldi A (1997) Geology of the NE Rift of Mount Etna, Sicily (Italy). *Acta Vulcanol* 9:91–100
- INGV (2002) List of Italian earthquakes (16–30 Sep, 2002). <http://www.ingv.it/~roma/reti/rms/bollettino/set0202/lista.htm>
- Kieffer G (1985) Évolution structurale et dynamique d'un grand volcan polygénique: stade d'édification et activité actuelle de l'Etna. PhD Thesis, Univ Clermont-Ferrand II, pp 1–497
- Lanzafame G, Neri M, Acocella V, Billi A, Funicello R, Giordano G (2003) Structural features of the July-August 2001 Mount Etna eruption: evidence for a complex magmatic system. *J Geol Soc Lond* 160:531–544
- Lo Giudice E, Rasà R (1992) Very shallow earthquakes and brittle deformation in active volcanic areas: the etnean region as an example. *Tectonophysics* 202:257–268
- McGuire WJ, Pullen AD (1989) Location and orientation of eruptive fissures and feeder-dykes at Mount Etna: influence of gravitational and regional stress regimes. *J Volcanol Geotherm Res* 38:325–244
- Neri M, Garduño VH, Pasquarè G, Rasà R (1991) Studio strutturale e modello cinematico della Valle del Bove e del settore nord-orientale etneo. *Acta Vulcanol* 1:17–24
- Neri M, Rossi M (2002) Geometria e volume dell'apparato vulcanico etneo: il contributo offerto dall'uso di mappe digitali. *Quad Geofis* 20:9–15 <http://www.ingv.it/~roma/cultura/biblioteca/biblioframe.html>
- Obrizzo F, Pingue F, Troise C, De Natale G (2001) Coseismic displacements and creeping along the Pernicana fault (Etna, Italy) in the last 17 years: a detailed study of a tectonic structure on a volcano. *J Volcanol Geotherm Res* 109:109–131
- Parfitt EA, Peacock DCP (2001) Faulting in the south flank of Kilauea volcano, Hawaii. *J Volcanol Geotherm Res* 106:265–284
- Patanè D (2002) Aggiornamento delle attività di monitoraggio sismico all'Etna. http://www.ct.ingv.it/report/Rapporto_eruzione_20021030.pdf
- Patanè D, De Gori P, Chiarabba C, Bonaccorso A (2003) Magma ascent and the pressurization of Mount Etna's volcanic system. *Science* 299:2061–2063 10.1126/science.1080653
- Pompilio M, Miraglia L, Corsaro RA (2002) I prodotti dell'eruzione di Ottobre 2002. Dati preliminari. <http://www.ct.ingv.it/Etna2002/Geo&Vulca/descprodotti30-10.htm>
- Pompilio M, Rutherford MJ (2002) Pre-eruption conditions and magma dynamics of recent amphibole-bearing Etna basalt (abs.) *Eos Trans AGU* 83(47) Fall Meet Suppl, F1419
- Rust D, Neri M (1996) The boundaries of large-scale collapse on the flanks of Mount Etna, Sicily. In: McGuire WJ, Jones AP, Neuberg J (eds) *Volcano instability on the Earth and other planets*. *Geol Soc Lond Spec Pub* 110:193–208
- Swanson DA, Duffield WA, Fiske RS (1976) Displacement of the south flank of Kilauea volcano: the result of forceful intrusion of magma into the rift zones. *US Geol Surv Prof Pap* 963, 39 pp
- Tanguy JC, Kieffer G (1993) Les éruptions de l'Etna et leurs mécanismes. *Mém Soc Géol Fr* 163:239–252
- Tibaldi A, Groppelli G (2002) Volcano-tectonic activity along structures of the unstable NE flank of Mt. Etna (Italy) and their possible origin. *J Volcanol Geotherm Res* 115:277–302
- Van Wyk de Vries B, Francis PW (1997) Catastrophic collapse at stratovolcanoes induced by slow volcano spreading. *Nature* 387:387–390
- Van Wyk de Vries B, Self S, Francis PW, Keszthelyi L (2001) A gravitational spreading origin for the Socompa debris avalanche. *J Volcanol Geotherm Res* 105:225–247
- Voight B, Glicken H, Janda RJ, Douglas PM (1981) Catastrophic rockslide avalanche of May 18. In: Lipman PW, Mullineaux DR (eds) *The 1980 eruptions of Mount St. Helens, Washington*. *Geol Surv Prof Pap* 1250:347–377